ACI STRUCTURAL JOURNAL TECHNICAL PAPER

Title no. 85-S27

Predicting the Response of Reinforced Concrete Beams Subjected to Shear Using Modified Compression Field Theory

by Frank J. Vecchio and Michael P. Collins

The recently developed modified compression field theory provides a unified approach to the analysis of reinforced concrete elements under general in-plane stress conditions. The concept and formulations of this theory can be extended to enable the analysis of reinforced concrete beams loaded in combined shear, moment, and axial load. Predictions of ultimate load capacity and complete load-deformation response of beams can thus be obtained.

An analytical model for the analysis of beams, based on the modified compression field theory, is described in the paper. A rigorous solution procedure is presented along with two alternative approximate procedures. Predictions of the model are compared with experimental results and are shown to predict behavior accurately. The capabilities of the model are also discussed in relation to currently available procedures.

Keywords: axial loads; **beams (supports)**; **compression**; moments; prestressed concrete; reinforced concrete; **shear strength**; tension.

Current design procedures for reinforced concrete beams in shear are largely based on the truss analogy developed by Ritter[1] and Morsch[2] nearly a century ago. The truss analogy proposes that a cracked reinforced concrete beam acts like a truss with parallel longitudinal chords, a web composed of diagonal concrete struts, and transverse steel ties (see Fig. 1). When shear is applied to this truss, the concrete struts are placed in compression, while tension is produced in the transverse ties and in the longitudinal chords. The force components in each can be determined by statics. In discussing the angle of inclination of the concrete struts θ, Morsch concluded that it was mathematically impossible to determine the slope but that 45 deg was a conservative assumption. The equation for the amount of transverse reinforcement required, arising from Morsch's assumption, became known as the truss equation for shear. It has formed the basis of many of the design procedures for shear used since.

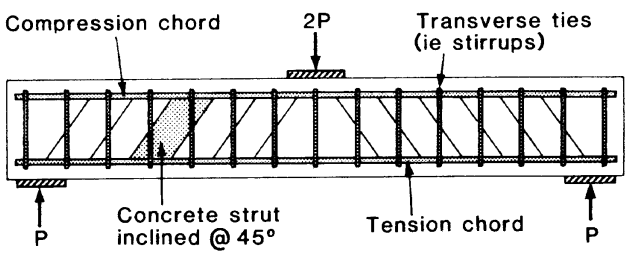

Fig. 1 — Truss analogy model for concrete beams in shear

Experience with the 45-deg truss analogy revealed that the results of this theory were typically quite conservative, particularly for beams with small amounts of web reinforcement. Consequently, it became accepted design practice in North America to add an empirical correction term to the truss equations. In the ACI Building Code (ACI 318-83),[3] this added shear capacity is taken as being equal to the shear at the commencement of diagonal cracking and is commonly referred to as the "concrete contribution." Various expressions for this concrete contribution have been produced to account for different loading situations and different types of members. These current design procedures for shear have been called "empirical mumbo jumbo."[4]

Recent years have seen a renewed interest among researchers concerning the behavior of reinforced concrete in shear. Much work has been directed toward formulating a more general model, free of empirical limitations. In particular, it was realized that the angle of inclination of the concrete struts θ was really only a part of the strain compatibility requirements that have to be satisfied together with the equilibrium requirements. The assumption that θ was equal to 45 deg was, in general, incorrect. Further, it was suspected that the

Received Sept. 24, 1986, and reviewed under Institute publication policies.
 Pertinent discussion will be published in the March-April 1989 *ACI Structural Journal* if received by Nov. 1, 1988.

ACI member ***Frank J. Vecchio*** *is an assistant professor in the Department of Civil Engineering at the University of Toronto, Ontario, Canada. He is on a leave of absence from Ontario Hydro, where he was a structural research engineer involved in the analysis and design of reinforced concrete nuclear power plant structures. Dr. Vecchio is a member of ACI Committee 435, Deflection of Concrete Building Structures, and of Canadian Standard Association CSA-N287.3, Technical Committee on Concrete Containment Structures for Nuclear Power Plants.*

Michael P. Collins, *FACI, is a professor of civil engineering at the University of Toronto. He is a member of joint ACI-ASCE Committee 445, Shear and Torsion, is chairman of the Canadian Standards Association Committee on Concrete Offshore Structures and a Canadian delegate to Comité Euro-International du Béton, and is a member of the Canadian Concrete Code Committee. He is also a member of ACI Committees 318, Standard Building Code; 358, Concrete Guideways; E901, Scholarships; and Subcommittee 318E, Shear and Torsion.*

behavior of the concrete struts, in terms of deformation and ultimate strength, was different than that of concrete loaded in uniaxial compression.

Much experimental and analytical research has been conducted recently at the University of Toronto toward formulating a more rational model. In particular, an extensive experimental program[5] was undertaken involving the testing of reinforced concrete panels under well defined general two-dimensional stress states, including shear. From the data acquired, the modified compression field theory[6] was developed. In this theoretical model, cracked concrete is treated as a new material with its own stress-strain characteristics. Equilibrium, compatibility, and constitutive relationships are formulated in terms of average stresses and average strains. Variability in the angle of inclination of the struts and strain-softening effects in the response of the concrete are taken into account. Consideration is also given to local stress conditions at crack locations. The resulting theory is capable of predicting accurately the response of reinforced concrete membrane elements subjected to in-plane shear and axial loads.

The concepts of the modified compression field theory can be applied to the analysis of reinforced concrete beams subjected to shear, moment, and axial load. Although too complex for regular use in the design of simple beams, the procedure has value in its ability to provide a rational method of analysis and design for members having unusual or complex geometry or loading, or whenever a more thorough analysis is warranted.

ANALYTICAL MODEL

The modified compression field theory relates average stresses to average strains in a cracked reinforced concrete element, satisfying conditions of compatibility and equilibrium. Unique states of stress and strain are assumed to exist in an element under load, as defined in Fig. 2. The strain conditions, both in the concrete and in the reinforcement, are summarized in the following relationship

$$\tan^2\theta = \frac{\epsilon_x - \epsilon_2}{\epsilon_y - \epsilon_2} = \frac{\epsilon_1 - \epsilon_y}{\epsilon_1 - \epsilon_x} \tag{1}$$

Similarly, the stress conditions in the concrete are related as follows

$$f_{cx} = f_{c1} - v_{cxy}/\tan\theta_c \tag{2}$$

$$f_{cy} = f_{c2} - v_{cxy} \cdot \tan\theta_c \tag{3}$$

and

$$f_{c1} = v_{cxy} \cdot (\tan\theta_c + 1/\tan\theta_c) \tag{4}$$

The stresses in the concrete, together with those in the reinforcement, must balance the external forces applied to the concrete element. A complete discussion is given in Reference 6.

Constitutive relations are required to determine the average stresses from the average strains. For concrete in compression, the relationship used is

$$f_{c2} = f_{c2max} \cdot \left| 2\left(\frac{\epsilon_2}{\epsilon_c'}\right) - \left(\frac{\epsilon_2}{\epsilon_c'}\right)^2 \right| \tag{5}$$

where

$$\frac{f_{c2max}}{f_c'} = \frac{1}{0.8 - 0.34\epsilon_1/\epsilon_c'} \leqslant 1.0 \tag{6}$$

For concrete in tension, prior to cracking, the relationship is

$$f_{c1} = E_c \cdot \epsilon_1 \tag{7}$$

where

$$E_c \simeq \frac{2f_c'}{\epsilon_c'} \tag{8}$$

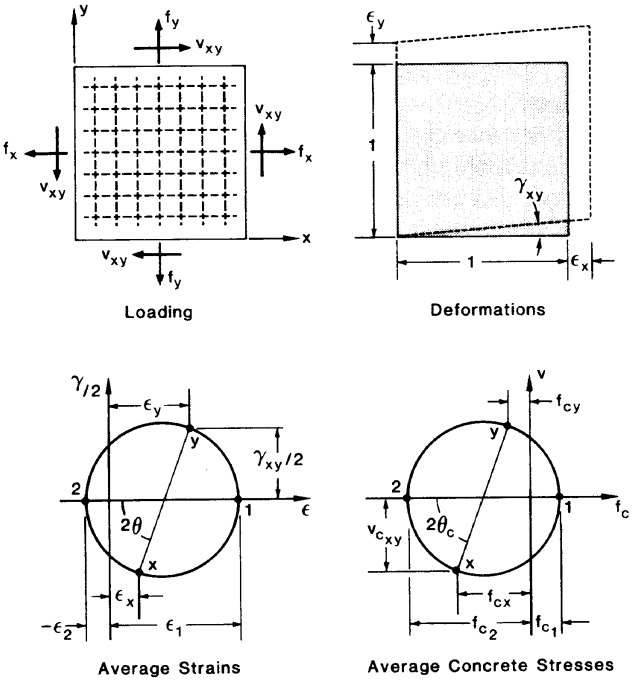

Fig. 2 — Average stress and strain conditions in a reinforced concrete element

The relationship suggested for response after cracking (i.e., tension stiffening effect) is

$$f_c = \frac{f_{cr}}{1 + \sqrt{200\epsilon_1}} \tag{9}$$

Further, it is assumed that the inclination of the principal stress coincides with that of the principal strain; that is, that

$$\theta = \theta_c \tag{10}$$

For the reinforcing steel, a bilinear uniaxial stress-strain relationship is adopted

$$f_s = E_s \cdot \epsilon_s \leqslant f_y \tag{11}$$

The constitutive relations are summarized in Fig. 3.

The previous formulations can be used in analyzing a reinforced or prestressed concrete beam by considering the beam to be composed of a series of concrete layers and longitudinal steel elements (see Fig. 4). Each concrete layer is then defined by its individual width b, depth h, amount of transverse reinforcement ρ_v, and position relative to the top of the beam y_c. The longitudinal steel elements are defined by their cross-sectional area A_s, initial prestrain $\Delta\epsilon_p$, yield strength f_{yx}, and position relative to the top of the beam y_s. Properties common to the entire beam cross section can include the concrete cylinder strength f'_c, concrete strain at peak stress ϵ'_c, yield strength of the transverse reinforcement f_{yv}, and Young's modulus for steel E_s. This layered model permits the analysis of beams having unusual cross-sectional shapes or reinforcing details.

The concrete layers and longitudinal steel elements are analyzed individually, although conditions of compatibility and equilibrium must be satisfied for the section as a whole. The only section compatibility requirement used is that plane sections remain plane. Thus, the longitudinal strain in each of the concrete layers and reinforcing bar elements will be fixed by defining the top and bottom fiber strains in the section, i.e.

$$\epsilon_{x_i} = \epsilon_t + \frac{(\epsilon_b + \epsilon_t)}{H} \cdot y_i \tag{12}$$

Force equilibrium requirements include: (1) a balancing of the shear, moment, and axial load acting on the section; and (2) horizontal shear equilibrium. Beyond this, uniform stress conditions are assumed to exist in each layer and element. Conditions of compatibility and equilibrium in the concrete layers are dictated by the modified compression field theory, and these also must be satisfied.

The analytical procedure requires that estimates be made of (1) the longitudinal strain distribution; and (2) the shear stress distribution across the section. Each individual concrete layer and reinforcing bar element can then be analyzed separately. The stresses in the longitudinal reinforcing bar elements can be determined directly from the longitudinal strains. For most analyses, a bilinear stress-strain relationship is adequate in determining the longitudinal steel stresses f_{sx}. The longitudinal stresses in the concrete layers are somewhat more difficult to determine. Given the longitudinal strain and normal shear stress acting on a particular layer, the remaining conditions of stress and strain must be determined according to the formulations of the modified compression field theory. In doing so, the concrete longitudinal compressive stress f_{cx} is found for each layer.

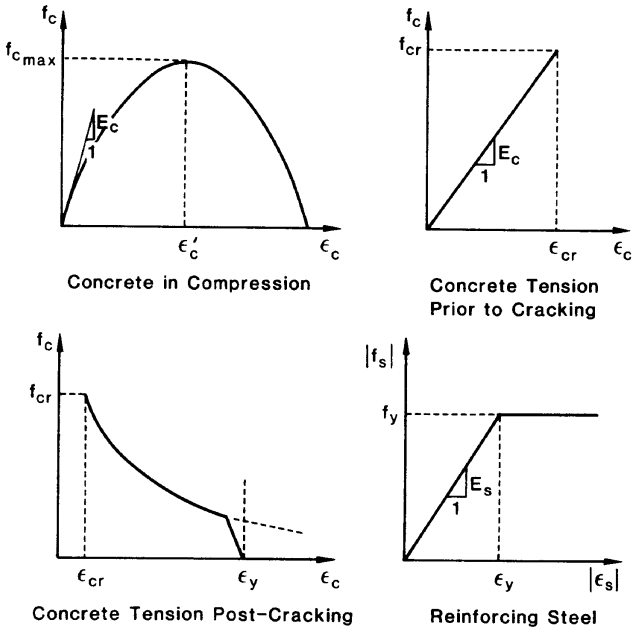

Fig. 3 — Constitutive relations for concrete and reinforcing steel

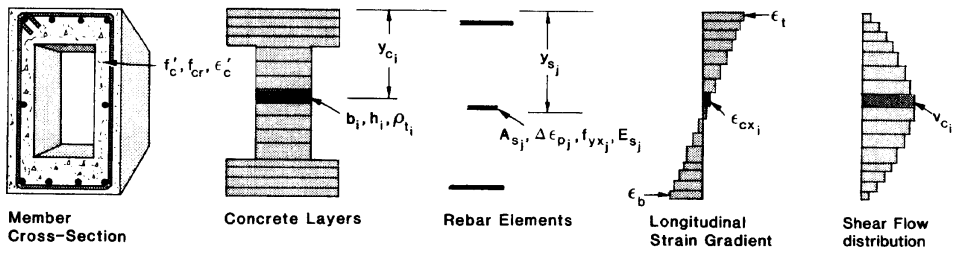

Fig. 4 — Beam section analyzed using layered model; estimates of longitudinal strain and shear flow distributions are required

Thus, for a given longitudinal strain and shear flow distribution, longitudinal stresses are determined for each of the concrete layers and reinforcing bar elements. The resultant of these stresses must balance the applied sectional forces. For a beam section discretized into m concrete layers and n longitudinal reinforcing bar elements, the elemental stresses must satisfy the following conditions

$$\sum_{i=1}^{m} f_{cxi} \cdot b_i \cdot h_i + \sum_{j=1}^{n} f_{sxj} \cdot A_{sj} = N \quad (13)$$

$$\sum_{i=1}^{m} f_{cxi} \cdot b_i \cdot h_i \cdot (y_{ci} - \bar{y}) + \sum_{j=1}^{n} f_{sxj} \cdot A_{sj} (y_{sj} - \bar{y}) = M \quad (14)$$

$$\sum_{i=1}^{m} v_{ci} \cdot b_i \cdot h_i = V \quad (15)$$

where N, M, and V are the axial load, moment, and shear acting about the centroid of the section. If the conditions are not satisfied, it becomes necessary to readjust the assumed longitudinal strain gradient and repeat the analysis until equilibrium is achieved.

The problem of determining the correct shear stress distribution is solved by analyzing a second section of the beam, a small distance removed from the first. Both sections are analyzed for the same shear stress distribution, satisfying section equilibrium in each case. The assumed shear stresses are then checked by examining the static equilibrium of each layer.

Let C_{i1} denote the compressive force acting on the face of concrete layer i at Section 1; C_{i2} denotes the force acting on the face at Section 2. Sections 1 and 2 are separated by a distance S (S is usually taken as about $H/6$). The compressive force C_i is determined primarily by the concrete longitudinal compressive stress. However, if a longitudinal reinforcing bar element is contained within the concrete layer, then the force in the reinforcing bar C_{si} must also be included. Thus

$$C_i = f_{cxi} \cdot b_i \cdot h_i + C_{si} \quad (16)$$

Now, consider concrete layer k, shown in Fig. 5. The horizontal shear forces acting on the layer F_{k-1} and F_k are determined as follows

$$F_{k-1} = \sum_{i=1}^{k-1} (C_{i1} - C_{i2}) \quad (17)$$

$$F_k = F_{k-1} + C_{k1} - C_{k2} \quad (18)$$

The normal shear force V_k can then be determined from rotational equilibrium of the free body shown in Fig. 5 as

$$V_k = \frac{(F_k + F_{k-1})}{2} \cdot \frac{h_k}{S} \quad (19)$$

Hence, the average shear stress acting on the vertical face of concrete layer k is calculated as

$$v_k = \frac{V_k}{b_k \cdot h_k} \quad (20)$$

The shear stresses calculated in the manner just described should correspond, in the case of each layer, to the shear stresses assumed initially. If they do not, then the assumed shear flow distribution must be revised and the analysis repeated.

The analytical procedure is schematically summarized in Fig. 6. A solution algorithm is given in Reference 5.

APPROXIMATE ANALYSES

Analyses conducted using the rigorous procedure just described have often shown the shear flow distributions in typical members to be fairly uniform across the area between the top and bottom reinforcement. This observation leads to a method of approximate analysis that allows for much quicker computation of section response. For a given beam cross section, an area of concrete extending between the centroids of the top and bottom reinforcement, and equal in width to the spalled web thickness, can be considered effective. Shear flows are then assumed to be uniformly distributed over this area. The subsequent steps in the solution procedure are identical to the more rigorous approach. But, by eliminating the iterations on shear flow estimates, the computational effort can be reduced by as much as an order of magnitude.

An alternative method of approximate analysis involves making an assumption regarding the normal shear strain through the depth of the section. Experience has shown that the shear strain through the section often varies in a nearly parabolic fashion, although it is highly dependent on the loading conditions and section details. If a parabolic shear strain distribution is assumed, then the analysis of a second section of

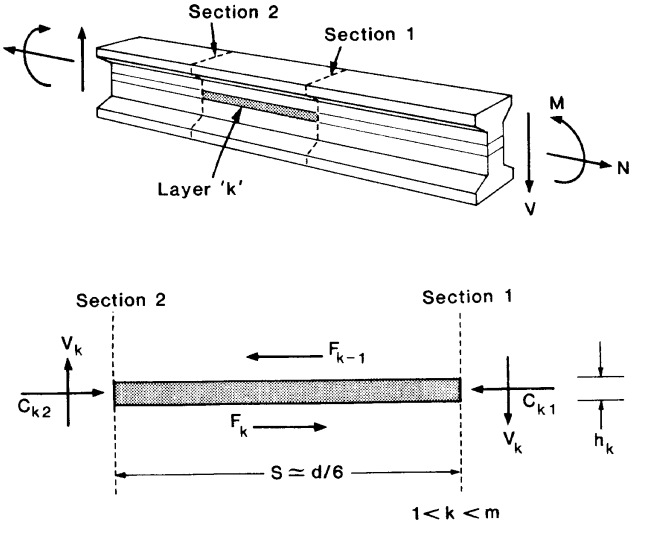

Fig. 5 — Free-body diagram for concrete layer k

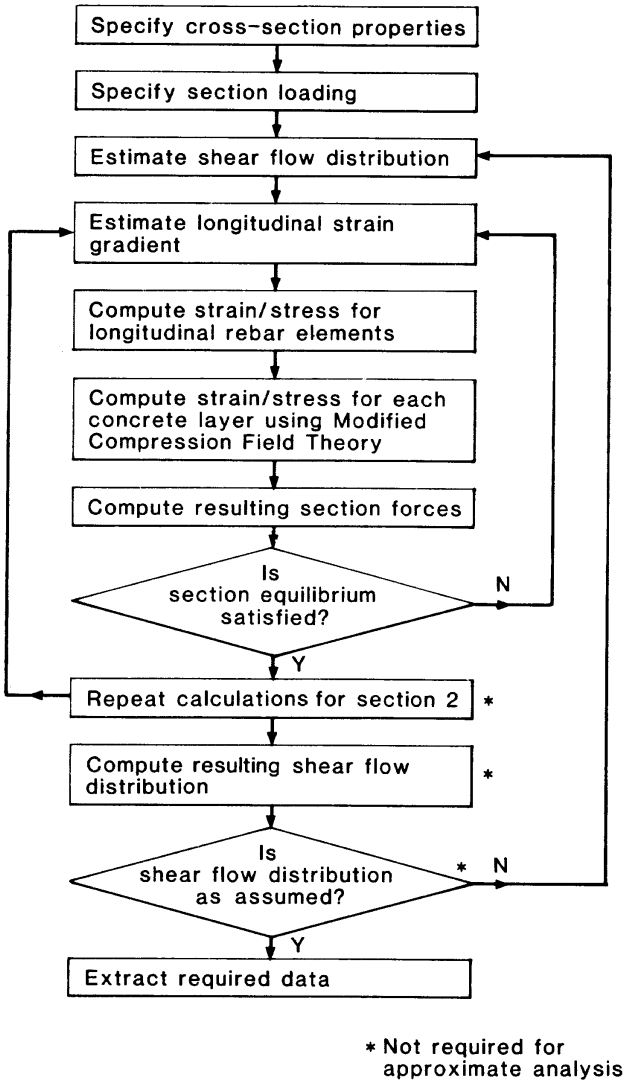

Fig. 6 — Solution procedure for beam analysis model

the beam can again be eliminated and computation time reduced. Further, if the complete shear force-deformation response curve is being computed for a beam, then the peak shear strain parameter (i.e., shear strain at the center of the section) can be monotonically increased and the resulting shear force calculated directly. This eliminates another set of iterative calculations and further speeds up computation.

To compare the relative accuracy of the two approximate methods to the more rigorous procedure, consider the interaction diagrams shown in Fig. 7. The interactions between shear capacity and flexural capacity for three typical beams are shown — a solid reinforced concrete beam, a hollow beam, and a prestressed T-beam. For each, the interaction curves were determined using all three analytical procedures.

In general, the approximate procedures give results that are fairly similar to those obtained using the more rigorous dual-section analysis. This is particularly true under conditions involving low flexure and axial loads. As the flexural moments increase, the predictions tend to diverge somewhat with the constant shear flow assumption generally yielding conservative results and the

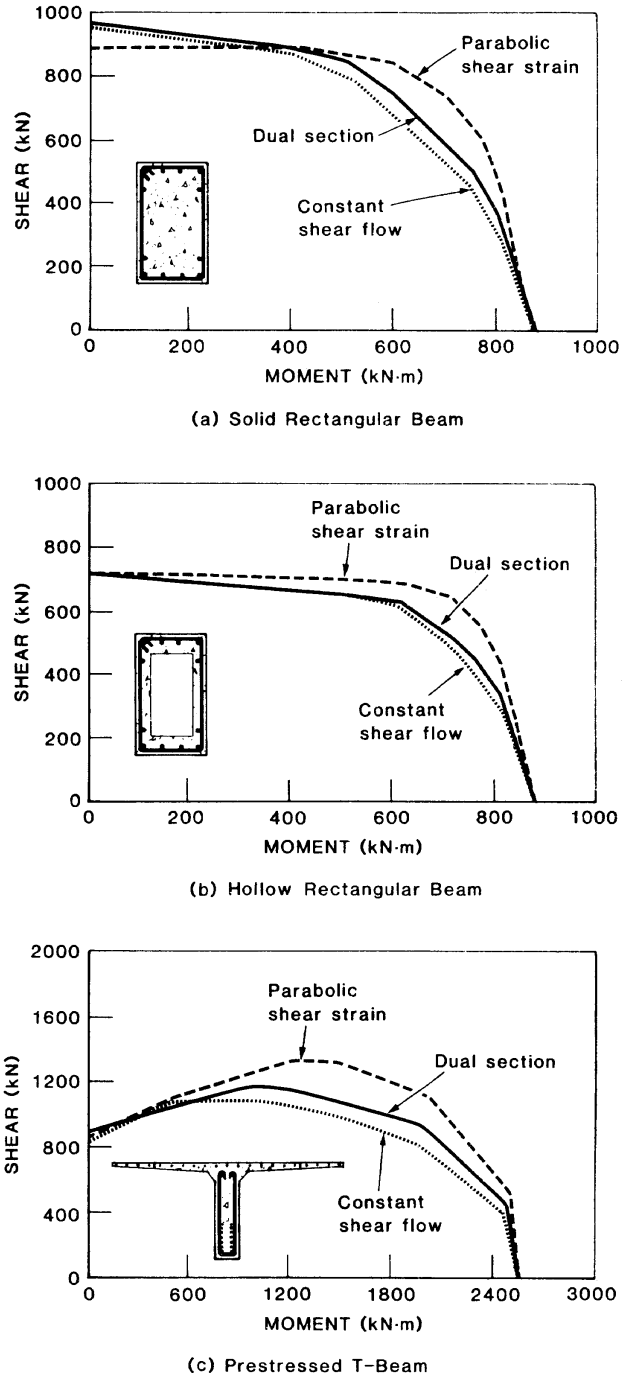

Fig. 7 — Moment-shear interaction diagrams comparing approximate procedures

parabolic shear strain assumption resulting in unconservative predictions. Inaccuracies obtained with the parabolic shear strain assumption are the result of an overestimated concentration of shear stress in the compression regions of the section. The constant shear flow assumption, on the other hand, overestimates the shear stresses in the tension regions, resulting in a weaker response. This is illustrated in Fig. 8, which shows the shear flow and strain distributions determined for a solid beam section [see Fig. 7(a)] when subjected to a shear force of 600 kN (135 kips) and a moment of 600 kN·m (442 ft-kips).

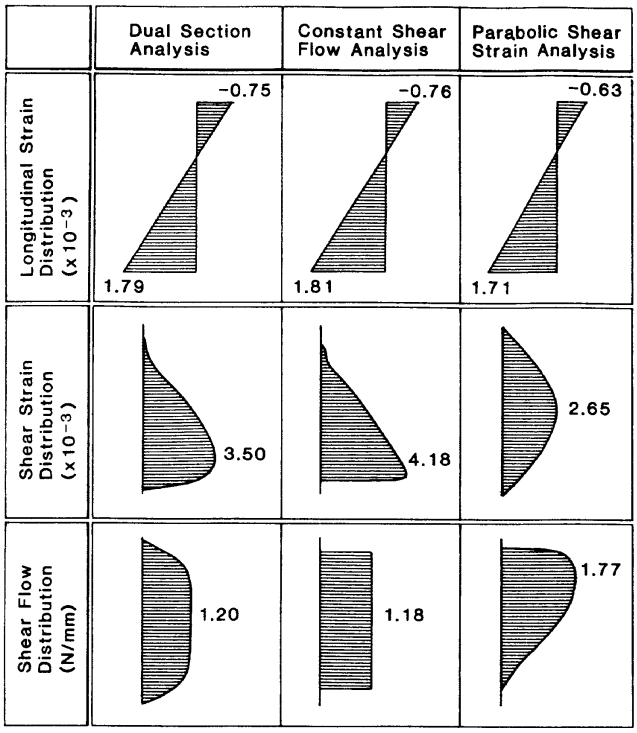

Fig. 8 — Shear flow and strain distribution for solid beam subjected to loads of V = 600 *kN and* M = 600 *kN·m*

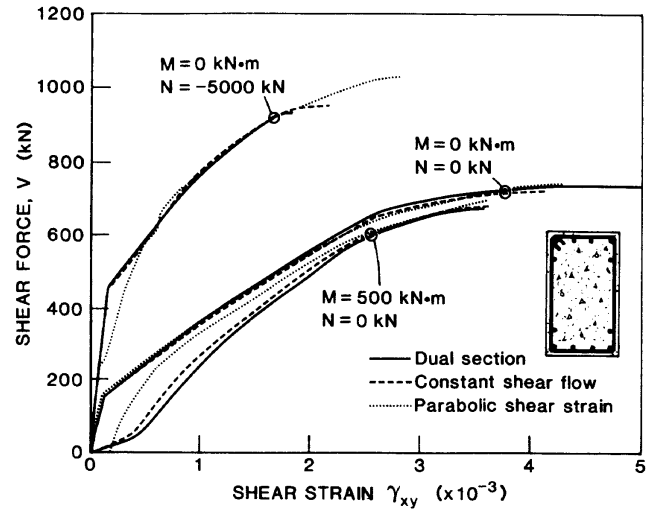

Fig. 9 — Shear load-deformation response of Beam SA3 obtained using alternative procedures

It should also be noted in Fig. 7 that, for the two symmetrically reinforced sections, all three methods predict that increasing the moment decreases the shear capacity. For the unsymmetrical T-beam, however, increasing the moment first results in an increase in shear strength. This is due to the flexural compression helping the weaker top flange resist the tensions caused by shear.

As well as being able to reasonably predict ultimate load, the approximate procedures give a fairly accurate prediction of load-deformation response. Fig. 9 shows the predicted load-deformation response curves for Beam SA3 (see Table 1) under three different loading conditions. In the case of pure shear, very little difference can be seen in the response computed using the three alternative methods. For the condition of combined shear and moment, the constant shear flow assumption results in slightly stiffer response, whereas the response computed using the parabolic shear strain assumption is significantly stiffer. Conversely, in the case of axial compression and shear, the parabolic shear strain assumption results in a lower cracking load and, consequently, a weaker shear stiffness in the intermediate load range.

COMPARISON WITH EXPERIMENTAL RESULTS

For corroboration, the analytical model was used to determine the theoretical response of several beams

Table 1 — Test beam properties

Beam	Dimensions		Concrete		Shear reinforcement			Longitudinal reinforcement		*P/S* reinforcement		
	Outside, mm	Void, mm	f'_c, MPa	ϵ'_c, $\times 10^{-3}$	Bars	S, mm	f_y, MPa	Bars	f_y, MPa	A_p, mm²	f_y, MPa	$\Delta\epsilon_p$, $\times 10^{-3}$
SA3	305 × 610	152 × 406	40.0	2.80	No. 3	72.4	373	12 - No. 9 4 - No. 7	345 462	—	—	—
SA4	305 × 610	152 × 406	40.0	2.80	No. 3	72.4	373	12 - No. 9 4 - No. 7	345 462	—	—	—
SK1	305 × 610	—	26.9	2.25	No. 3	100	400	8 - No. 8	442	1540	1450	4.82
SK2	305 × 610	121 × 381	26.9	2.25	No. 3	100	400	8 - No. 8	442	1540	1450	4.82
SK3	305 × 610	—	28.2	2.20	No. 3	100	400	8 - No. 8	442	—	—	—
SK4	305 × 610	121 × 381	28.2	2.20	No. 3	100	400	16 - No. 8	442	—	—	—
SP0	305 × 610	152 × 406	25.0	2.30	No. 3	150	373	16 - No. 8	421	—	—	—
SP1	305 × 610	152 × 406	33.5	2.30	No. 3	150	373	12 - No. 7	421	510	1450	4.21
SP2	305 × 610	152 × 406	32.0	2.00	No. 3	150	373	12 - No. 7	421	1010	1450	4.11
SP3	305 × 610	152 × 406	32.2	2.00	No. 3	150	373	12 - No. 7	421	1520	1450	4.26
SM1	305 × 610	152 × 406	29.0	2.40	No. 3	175	424	12 - No. 7	452	—	—	—
CF1	305 × 610	152 × 406	38.6	3.00	No. 3	150	367	6 - No. 3	367	930	1450	5.17

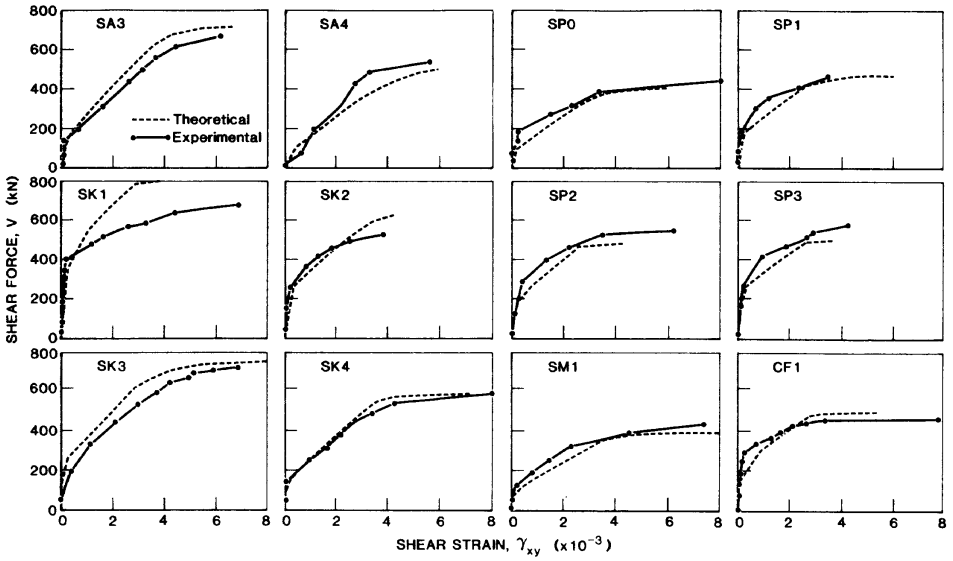

Fig. 10 — Comparison of predicted and measured load-deformation response of University of Toronto beams

tested by various researchers at the University of Toronto.[5] The beams selected for investigation were those that failed primarily due to the action of high shear stresses. All were 12 by 24 in. (305 by 610 mm) in cross section. Section designs ranged from solid to hollow, from prestressed to nonprestressed. Several different test methods were used to apply load but, in all cases, the moment was zero at the midpoint of the test length of the beam. In addition, all of the beams were well instrumented and detailed strain readings were taken during the testing. The material and section properties for the 12 specimens considered are summarized in Table 1.

For the theoretical analyses, spalled web dimensions (to the outside of the stirrups) were used throughout. In the cases where prestressing ducts were present, one-half of the width of the duct was subtracted from the web width for the layer containing the duct. The analytical results were compared to the experimental data for the central regions of each test specimen where the moments were close to zero.

The theoretical and experimental shear response curves for each specimen are compared in Fig. 10. In general, it can be seen that the experimental and theoretical response curves agree well. Precracking, postcracking, and ultimate load-deformation response are well modeled, particularly for those specimens that were not precracked prior to testing. Specimens SK1 and SK2 were the least accurately predicted. These beams failed at loads about 15 percent less than the predicted capacities, with severe crushing and spalling of concrete over the prestressing ducts evident. The concrete elsewhere in the beams was relatively undamaged. For these beams, the practice of partially reducing the effective width of the webs did not completely account for the detrimental effects caused by the smooth, rigid steel tubes used as ducts.

Fig. 11(a) compares the theoretical and experimental ultimate shear strengths for the Toronto specimens, showing good correlation between the two. The ratio of experimental to theoretical strengths has a mean of 1.01 and a coefficient of variation of 9.9 percent.

An extensive series of beam shear tests was conducted by Haddadin, Hong, and Mattock[7] at the University of Washington. The beam specimens tested were T-sections, simply supported and with constant axial loads applied at the ends. Shear loads were introduced through single-point loading at midspan. Variables included the span length, the shear reinforcement ratio, and the level of axial force applied. Thirty-five specimens are reported in the Series I test program. These specimens were analyzed using the analytical procedure described, and the predicted ultimate strengths are compared to the experimental values in Fig. 11(b). In general, very good agreement is obtained. The ratio of experimental to predicted strength has a mean of 1.01 and a coefficient of variation of 15 percent. If the six beams that did not contain shear reinforcement are excluded, then the ratio of experimental to predicted strength has a mean of 1.04 and a coefficient of variation of 9.3 percent.

Elzanaty, Nilson, and Slate[8] report tests conducted at Cornell University involving beams constructed from high-strength concrete. Two series of tests are reported, one involving beams having a T-section and the other an I-section. In both cases, high axial compressive stresses were induced through prestressing. Concrete strengths ranged from 40 to 74 MPa (5800 to 10,700 psi). Other variables included percentage of transverse reinforcement and amount of prestressing force. All beams were simply supported, and subjected to a two-point loading with a shear span of 1.2 m. The ultimate strengths predicted for these beams, based on the modified compression field theory formulations,

are compared with the experimental results in Fig. 11(c). The ratio of the experimental to predicted strengths obtained has a mean of 0.94 and a coefficient of variation of 4.4 percent. It should be noted, however, that in making the theoretical calculations, the tensile strength of the concrete was assumed to be $0.33\sqrt{f'_c}$ MPa ($4\sqrt{f'_c}$ psi). For high-strength concrete, this was likely an overestimation of cracking strength and, thus, contributed to the consistently high predicted strengths. For Beam CI 17, for example, a predicted shear strength of 138 kN (31.0 kips) was obtained using $f_{cr} = 0.33\sqrt{f'_c}$ MPa, whereas a reanalysis using $f_{cr} = 0.17\sqrt{f'_c}$ MPa ($2\sqrt{f'_c}$ psi) resulted in a theoretical shear strength of 120 kN (27.0 kips). The experimentally obtained value was 129.5 kN (29.1 kips).

The analytical procedure has been shown to give good results in the experimental studies just described, as well as others involving a wide range of section details and loading conditions. However, it must be remembered that the response of reinforced concrete in shear inherently involves a wide scatter and that high accuracy in prediction of strength should not be expected or relied upon. Consider, for example, beam specimens CI 12 and CI 15 reported in Reference 8. The beam details and loading conditions were identical except that the strength of the concrete in Beam CI 15 was much higher — 70.4 MPa (10,200 psi) as compared to 40 MPa (5800 psi) for Beam CI 12. Beam CI 12 had an ultimate shear strength of 122.4 kN, whereas Beam CI 15, surprisingly, was lower at 121.0 kN. In all other tests of this series, a higher concrete strength resulted in a higher shear strength. As a further illustration, consider the beam specimens reported in Reference 9, which were loaded in combined shear, flexure, and high axial compression. The ultimate strengths attained were in some cases considerably higher than the nominal strengths of the members subjected to flexure and axial force alone.

CAPABILITIES AND APPLICATION

The analytical procedure presented enables rational and comprehensive analyses of reinforced concrete sections subjected to combined flexure, shear, and axial load to be performed. The procedure incorporates compatibility and equilibrium conditions and utilizes realistic stress-strain relationships for cracked reinforced concrete. The model inherently takes into account the softening of the concrete in compression and the stiffening effects of cracked concrete in tension, both major influencing factors. Because of the layered approach used, the procedure is applicable in the analysis of members with irregular cross sections. For example, it has been used with extremely good results in the analysis of circular columns tested under high shear.[10] Further, the analyses provide complete data regarding the load-deformation response, including stress and strain conditions in the concrete, longitudinal reinforcement, and transverse reinforcement at any location in the cross section. The shear stress distribution over the cross section is determined as well. The ana-

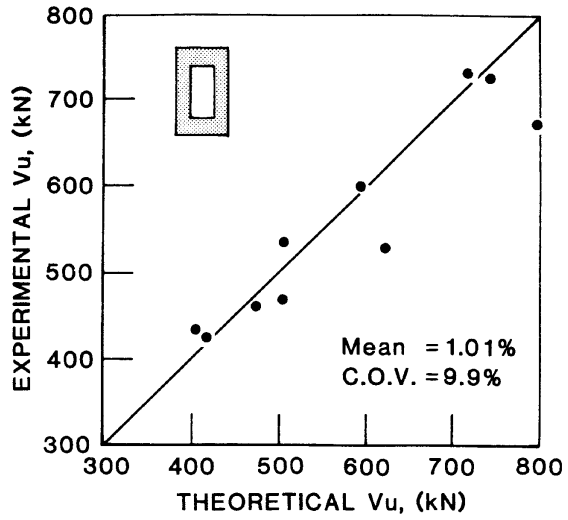

(a) University of Toronto Tests

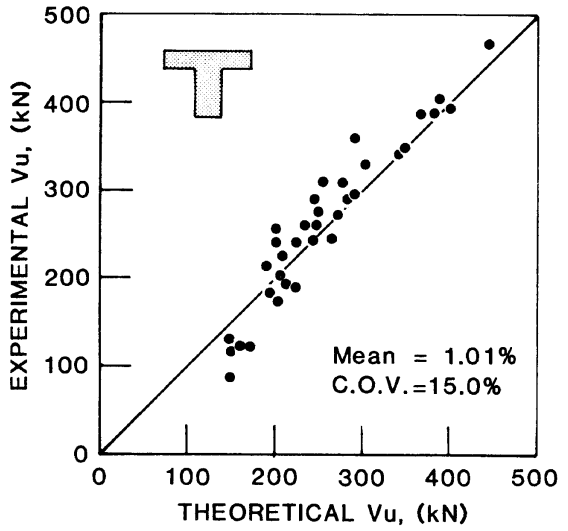

(b) University of Washington Tests

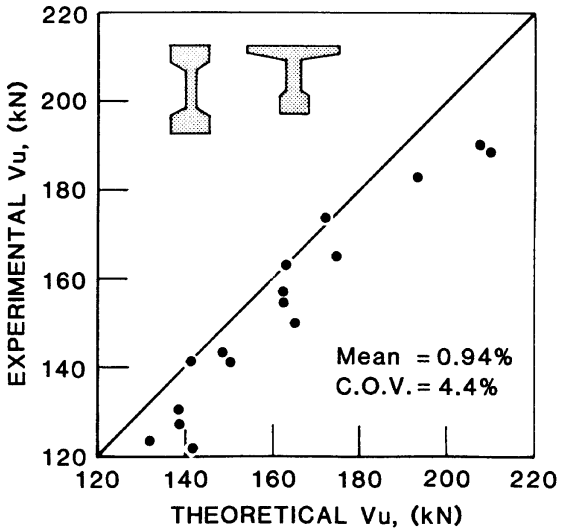

(c) Cornell University Tests

Fig. 11 — Correlation of experimental to theoretical shear strengths of three beam test series

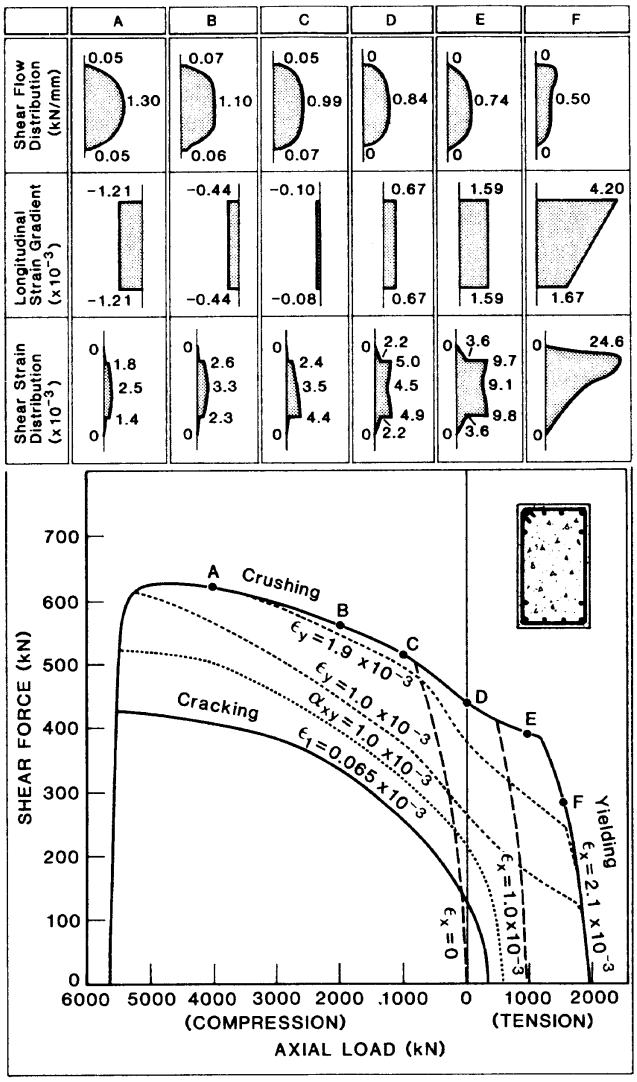

Fig. 12 — Shear-axial load interaction diagram showing various aspects of response

lytical model can be applied to a wide range of cross sections and reinforcing and loading situations, including members without shear reinforcement. In all of these respects, the procedure is superior to the empirical formulations currently in use.

As an illustration of the capabilities of the procedure, an analysis was performed of Beam SPO (see Table 1 for details). Fig. 12 shows the shear-axial force interaction diagram determined for the case of zero moment of this beam. As can be seen, axial compression considerably increases the ultimate shear capacity of the section in the absence of high flexural loads. This pattern of behavior was confirmed in the tests conducted by Mattock and Wang.[9] Axial tensile forces, as expected, result in a significant decrease in shear strength. Also shown in Fig. 12 are the cracking load envelope and the peak strains in the stirrups ϵ_y and longitudinal reinforcement ϵ_x at various load combinations. The longitudinal strain and the shear flow distributions, at various points along the ultimate load envelope, are illustrated also. The shear flows are fairly uniform between the longitudinal reinforcing bars for

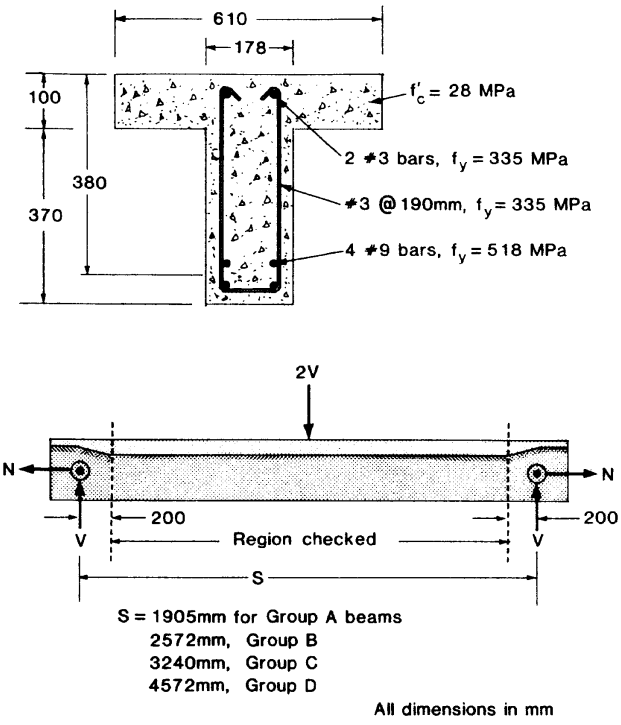

Fig. 13 — Cross section and loading details for University of Washington test beams[7]

conditions of pure shear or shear and tension. However, as axial compression increases, the shear flow tends to have a more rounded profile. The same is true of the shear strain distribution. In beam sections with high flexural loads, the shear flows are concentrated toward the compression flange.

The analytical procedure described in this paper enables the response of a section of a beam to be predicted. In predicting the response of an actual beam, different sections along the length of the beam may have to be checked. To illustrate this point, consider 12 of the T-beams tested by Haddadin, Hong, and Mattock.[7] As shown in Fig. 13, these beams were supported on axles projecting from circular bearing plates bolted to the beams. As well as providing vertical support, the axles were used to apply axial load to the beams. All 12 beams had the same sectional properties but differed in their span lengths and in the applied axial loads.

Fig. 14 gives the shear-moment interaction diagrams for the three different levels of axial load used in Haddadin, Hong, and Mattock's tests. Because the section used was very unsymmetrically reinforced, a section with zero moment is predicted to be considerably weaker than one with a substantial moment. The sections with applied tension are predicted to be particularly weak in regions of low moment, with the failure being initiated by yielding of the top longitudinal reinforcement.

Also shown in Fig. 14 are 12 horizontal lines that represent the combinations of shear and moment at failure for each of the 12 beams. Along the test length the shear is constant but the moment increases. As the

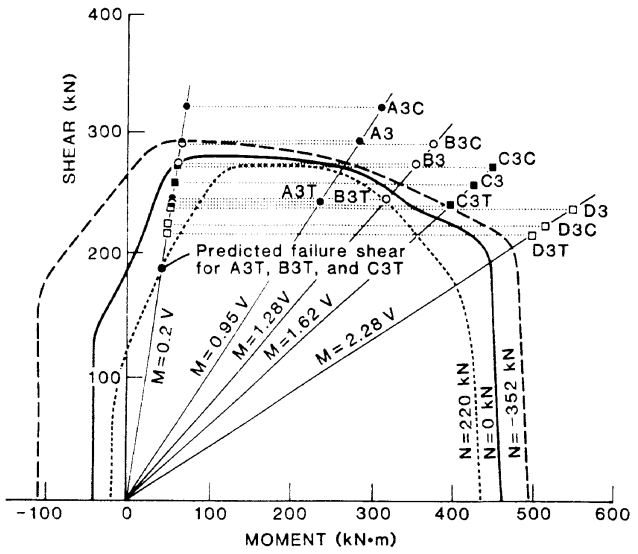

Fig. 14 — Shear-moment interaction diagram for University of Washington test beams

load on a given beam is increased, the line representing the shears and moments along the test length goes higher. Failure is predicted to occur when one end of the line reaches the failure envelope (i.e., the interaction diagram). Thus, Beams A3T, B3T and C3T, which have three different spans, are all predicted to fail at the same shear because the failures occur near the support. On the other hand, Beams A3C, B3C, C3C and D3C are predicted to fail at different shears with the failure shear becoming smaller as the spans become longer. It can be seen that the analytical model predicts well the observed experimental trends.

Because the analytical procedure is a sectional model that assumes that plane sections remain plane, it is not capable of predicting the local effects caused by the support and the loading details. Thus, the beneficial effects of the transverse compressive stresses introduced by the support are ignored. As a result, the method will typically underestimate the shear capacity of regions where a significant portion of the load is carried by direct strut action. To predict the response of such regions, models that use more complete compatibility conditions (e.g., Reference 11) need to be employed.

CONCLUSIONS

The modified compression field theory enables realistic predictions of the response of reinforced concrete membrane elements subjected to in-plane shear and axial forces to be made. It is formulated to satisfy general conditions of compatibility and equilibrium while incorporating realistic constitutive relations for cracked concrete in tension and in compression, as determined from extensive test data. Strain softening and tension stiffening effects, critical factors in determining the response of concrete to shear, are intrinsically taken into account.

In this paper, the concepts of the modified compression field theory have been incorporated into an analytical model for analyzing the response of reinforced or prestressed concrete beams under combined shear, moment, and axial loads. The analytical model developed, based on a layered representation of the beam cross section and involving an iterative solution procedure for longitudinal strains and shear stress distributions, allows analysis of unusual or complex beam sections under wide-ranging load conditions. Various influencing factors can also be treated in a rational manner. In cases where more approximate solutions will suffice, simplifying assumptions can be made that substantially reduce the computational effort required. Predictions based on this model have been shown to agree well with experimental results.

The proposed model provides an enhanced ability to design and analyze the shear response of beams in a rational manner, rather than having to rely on restrictive, narrow-ranging and often overly conservative empirical formulations. The method is seen as being most useful in situations where economic or technical considerations warrant that a more thorough analysis be performed than is otherwise obtainable using standard code procedures.

ACKNOWLEDGMENTS

The modified compression field theory, and its adaptation to beam analysis, was the result of research funded by a series of grants from the Natural Sciences and Engineering Research Council of Canada and grants from Ontario Hydro. The authors would like to express their gratitude to these organizations for their support. The analytical predictions summarized in Fig. 7 were prepared by Ms. Gabrielle Zapf, research assistant; her efforts are much appreciated.

NOTATION

A_{ps} = cross-sectional area of prestressing steel
A_s = cross-sectional area of longitudinal reinforcing bar element
b = width of concrete layer
C = compressive force acting on layer face
C_s = compressive force acting in longitudinal bar
E_c = modulus of elasticity of concrete
E_s = modulus of elasticity of reinforcing steel
f'_c = maximum compressive stress observed in a cylinder test (negative quantity)
f_{c1} = principal tensile stress in concrete
f_{c2} = principal compressive stress in concrete
f_{cr} = concrete cracking stress
f_{cx} = stress in concrete in longitudinal direction
f_{cy} = stress in concrete in transverse direction
f_s = stress in reinforcement
f_{sx} = stress in longitudinal reinforcement
f_{sy} = stress in transverse reinforcement
f_y = yield stress of reinforcement
f_{yx} = yield stress of longitudinal reinforcement
f_{yy} = yield stress of transverse reinforcement
F = shear force on layer surface
h = depth of concrete layer
H = total depth of beam cross section
M = moment acting on beam section
N = axial force acting on beam section
S = spacing between beam cross sections
v_{cxy} = shear stress on concrete layer face

V = shear force acting on beam section
y = distance from top of beam section
$\bar{y}$ = distance from top to centroid of section
ϵ_1 = principal tensile strain in concrete
ϵ_2 = principal compressive strain in concrete (negative quantity)
ϵ_b = bottom fiber strain in beam section
ϵ_c' = strain in concrete cylinder at peak stress f_c' (negative quantity)
ϵ_s = strain in reinforcement
ϵ_t = top fiber strain in beam section
ϵ_x = strain in longitudinal direction
ϵ_y = strain in transverse direction
θ = angle of inclination of principal strains
θ_c = angle of inclination of principal stresses in concrete
ρ_y = reinforcement ratio for steel in transverse direction
$\Delta\epsilon_p$ = difference between strain in prestressing tendon and strain in an adjacent fiber of concrete

REFERENCES

1. Ritter, W., "Die Bauweise Hennebique," *Schweizerische Bauzeitung* (Zürich), Feb. 1899.

2. Mörsch, Emil, *Concrete-Steel Construction* (Der Eisenbetonbau), English translation of the 3rd German edition, McGraw-Hill Book Co., New York, 1909, 368 pp.

3. ACI Committee 318, "Building Code Requirements for Reinforced Concrete (ACI 318-83)," American Concrete Institute, Detroit, 1983, 111 pp.

4. MacGregor, J. G., "Challenges and Changes in the Design of Concrete Structures," *Concrete International: Design & Construction,* V. 6, No. 2, Feb. 1984, pp. 48-52.

5. Vecchio, F. J., and Collins, M. P., "The Response of Reinforced Concrete to In-Plane Shear and Normal Stresses," *Publication* No. 82-03, Department of Civil Engineering, University of Toronto, Mar. 1982, 332 pp.

6. Vecchio, Frank J., and Collins, Michael P., "The Modified Compression-Field Theory for Reinforced Concrete Elements Subjected to Shear," ACI JOURNAL, *Proceedings* V. 83, No. 2, Mar.-Apr. 1986, pp. 219-231.

7. Haddadin, Munther J.; Hong, Sheu-Tien; and Mattock, Alan H., "Stirrup Effectiveness in Reinforced Concrete Beams with Axial Force," *Proceedings,* ASCE, V. 97, ST9, Sept. 1971, pp. 2277-2297.

8. Elzanaty, Ashraf H.; Nilson, Arthur H.; and Slate, Floyd O., "Shear Capacity of Prestressed Concrete Beams Using High-Strength Concrete," ACI JOURNAL, *Proceedings* V. 83, No. 3, May-June 1986, pp. 359-368.

9. Mattock, Alan H., and Wang, Zuhua, "Shear Strength of Reinforced Concrete Members Subjected to High Axial Compressive Stress," ACI JOURNAL, *Proceedings* V. 81, No. 3, May-June 1984, pp. 287-298.

10. Khalifa, J. U., and Collins, M. P., "Circular Reinforced Concrete Members Subjected to Shear," *Publication* No. 81-08, Department of Civil Engineering, University of Toronto, Dec. 1981, 103 pp.

11. Adeghe, L. N., "A Finite Element Model for Studying Reinforced Concrete Detailing Problems," PhD thesis, Department of Civil Engineering, University of Toronto, 1986.

Authorized Reprint From
May/June 1988, issue of
Structural Journal
Published by American Concrete Institute